Advances in Water Resources 51 (2013) 292–304

Contents lists available at SciVerse ScienceDirect

Advances in Water Resources

journal homepage: www.elsevier.com/locate/advwatres

Biological constraints on water transport in the soil–plant–atmosphere system

Stefano Manzoni *, Giulia Vico, Amilcare Porporato, Gabriel Katul

Department of Civil and Environmental Engineering, Box 90287, Duke University, Durham, NC 27708-0287, USA
Nicholas School of the Environment, Box 90328, Duke University, Durham, NC 27708, USA

ARTICLE INFO

Article history:
Available online 30 March 2012

Keywords:
Soil–plant–atmosphere continuum
Transpiration
Vulnerability to cavitation
Water potential
Plant trait
Hydraulic conductivity

ABSTRACT

An effective description of water transport in the soil–plant–atmosphere continuum (SPAC) is needed for wide-ranging applications in hydrology and climate-vegetation interactions. In this contribution, the theory of water movement within the SPAC is reviewed with emphasis on the eco-physiological and evolutionary constraints to water transport. The description of the SPAC can be framed at two widely separated time scales: (i) sub-hourly to growing season scales, relevant for hydro-climatic effects on ecosystem fluxes (given a set of plant hydraulic traits), and (ii) inter-annual to centennial scales during which either hydraulic traits may change, as individuals grow and acclimate, or species composition may change. At the shorter time scales, water transport can be described by water balance equations where fluxes depend on the hydraulic features of the different compartments, encoded in the form of conductances that nonlinearly depend on water availability. Over longer time scales, ontogeny, acclimation, and shifts in species composition in response to environmental changes can impose constraints on these equations in the form of tradeoffs and coordinated changes in the hydraulic (and biochemical) parameters. Quantification of this evolutionary coordination and the related tradeoffs offers novel theoretical tactics to constrain hydrologic and biogeochemical models.

1. Introduction

Water transport through soil, vegetation, and the atmosphere typically constitutes the largest hydrologic output in most terrestrial systems. On the one hand, soil properties and plant activity influence the partitioning of rainfall into evapotranspiration, runoff, and deep percolation, thus impacting the regional-scale water balance. On the other hand, transpiration is tightly coupled to the carbon cycle through simultaneous exchanges of CO_2 and water via the stomatal pathway, thus ultimately controlling C uptake by vegetation and affecting long-term C storage in ecosystems. Because of these fundamental roles, water movement through the soil–plant–atmosphere continuum (SPAC) remains a subject of active research in hydrology and plant and agricultural sciences, and a key topic in any assessment of elemental cycling in natural and agro-ecosystems, under current and future climate scenarios. Moreover, because terrestrial plants are first users of precipitated water, they directly affect the recharge of water systems: as such, their impact on water resources cannot be ignored.

Quantifying water movement through the SPAC requires understanding water dynamics in three main compartments (soil, plant tissues, and atmosphere) and through the interfaces and connections among them (soil–root interface and leaf surface). The driving force for water movement is provided by the gradient in total water potential between the soil and the atmosphere [1,2], which causes liquid water to move from the soil into the plant and then to evaporate and diffuse from the mesophyll and epidermal cells through the stomata (also directly through the cuticle) and into the atmosphere [3]. By means of guard cell movements, which alter the size of the stomatal aperture, plants are able to regulate water losses through transpiration at the most effective location, i.e., where the steeper water potential gradient develops between the nearly saturated stomatal cavity and the atmosphere [4]. The flux of liquid water through the soil and plant tissues takes place under high tension, and is generally framed within the context of cohesion–tension theory [5–9].

Quantitatively describing this water flux is complicated by incomplete knowledge of microscopic-scale processes, the large spatial heterogeneity of the transporting medium (e.g., root and branch architecture), and the temporal variability of the external drivers [10,11]. Because of these intrinsic complexities, simplified models that capture the macroscopic dynamics through mass balance equations are a viable alternative to a detailed representation of the micro-scale processes. Following this simplified approach and in the context of cohesion–tension theory, the flux of liquid water is often described by an electrical analogy, where water encounters a series of resistances (or conductances) from the soil

* Corresponding author at: Department of Civil and Environmental Engineering, Box 90287, Duke University, Durham, NC 27708-0287, USA. Tel.: +1 919 6605467; fax: +1 919 6605219.
E-mail address: stefano.manzoni@duke.edu (S. Manzoni).

0309-1708/$ - see front matter © 2012 Elsevier Ltd. All rights reserved.
http://dx.doi.org/10.1016/j.advwatres.2012.03.016

to the leaves together with decreased gravitational potential with elevation [2,4,6,12–14]. A price to pay for such simplified macroscopic view of the dynamics within the SPAC is a high degree of nonlinearity in conductances with respect to water potential. In fact, conductances in both the soil and the plant tissues are known to be nonlinearly related to water potential (or water saturation; see Fig. 1): such nonlinearities are caused by air entry and reduction of liquid water films in soils [12,15,16] and the occurrence of cavitation in the xylem [9,17]. Similarly, stomatal conductance declines nonlinearly as water potential decreases, besides changing as a function of other environmental and biochemical factors [18–21].

Much work on the soil–plant system has focused on describing water fluxes when a given set of plant characteristics are known, and where the time scales are those imposed by soil drying, stomatal control, and cavitation development (sub-hourly to the growing season). However, the various components of the SPAC respond to environmental changes also over longer time scales, at which individuals acclimate and grow, and species composition changes [22,23]. Thus, especially in the face of climatic changes, it is becoming necessary to assess how these hydraulic features are altered at longer time scales in both individuals and at the ecosystem level. In this contribution, such two time scales are explored exploiting their large time scale separation. First, a simplified framework for a short-term description of water flow is presented, assuming static plant traits. Spatially explicit representations are simplified to provide lumped 'macroscopic' equations primarily intended to illustrate the role of mechanisms and plant characteristics. These lumped equations are applicable and testable using quantities commonly measured at the macro-scale (e.g., soil cores, leaves, and stem segments, up to field-scale flux measurements), which are becoming readily available through published global databases (e.g., TRY, [24], FLUXNET, [25]). Next, coordinated changes of plant hydraulic characteristics in response to environmental variations during ontogeny or succession are explored. From a practical perspective, such coordination between traits necessarily implies a set of constraints that can be formulated as linkages between the various elements of the soil–plant hydraulic apparatus, and between the hydraulic and photosynthetic machinery of the plant itself. From the point of view of plant function, coordination among plant conductances improves the hydraulic efficiency along the SPAC [26–30], and the scaling of water supply with leaf photosynthetic capacity optimizes resource use [31–35]. Plant form also results from evolutionary tradeoffs between structural and functional constraints [36], leading to optimal branching networks and xylem vessel size [34,37,38]. After discussing how these optimality criteria are used to relate the key hydraulic characteristics of plants to each other, the review concludes with future research priorities necessary for implementing such biological constraints on the dynamics of water in the SPAC.

2. Governing equation for water transport through the SPAC

As a starting point, horizontal homogeneity is assumed so that the focus is only on vertical transport of water from the soil to the atmosphere. To describe water transport within a common framework, total water potential is employed as a natural unit to

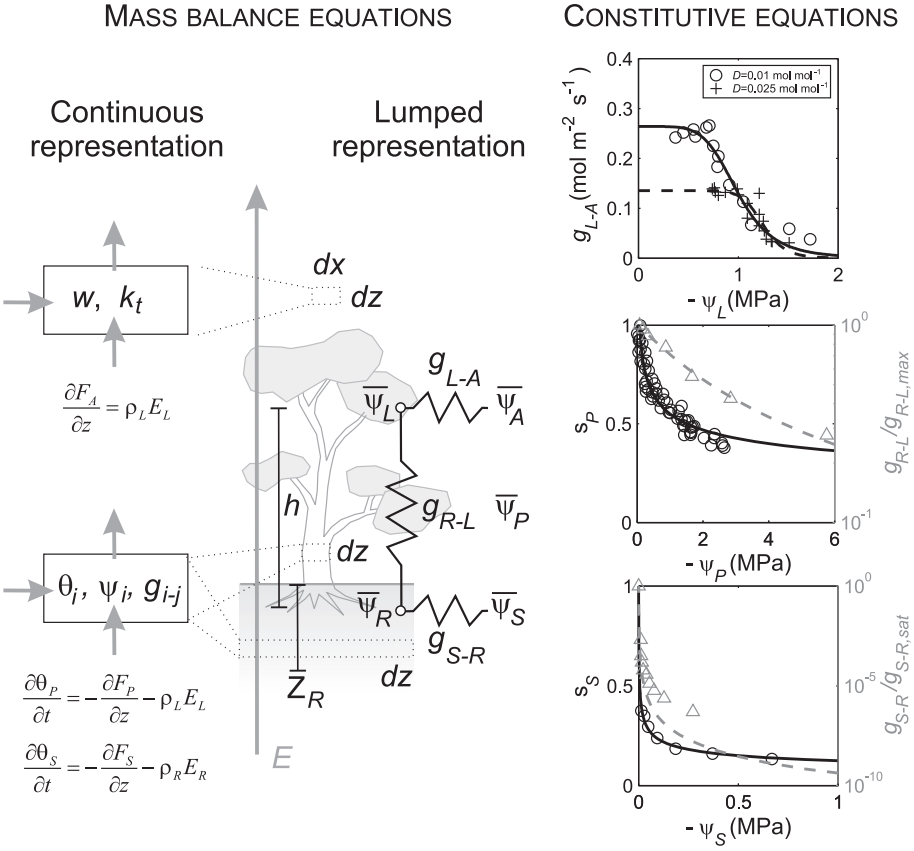

Fig. 1. General scheme of the soil–plant–atmosphere continuum (SPAC): illustration of the mass balance in the continuous and lumped representations and constitutive equations for water flow through soil (subscript *S*), plant xylem (subscript *P*), and atmosphere (subscript *A*). Top, stomatal conductance ($g_{L\text{-}A}$ for well ventilated conditions) as a function of leaf water potential at two contrasting vapor pressure deficits (*D*) in *Nerium oleander* [178]; middle, water retention curve (black) and vulnerability to cavitation (gray) of *Tapiria guianensis* branches [63]; bottom, water retention and hydraulic conductivity data and curves (Eqs. (5) and (9)) for a sandy loam soil (black and gray, respectively)[46].

characterize water content in the different compartments of the SPAC (Fig. 1). It is the continuity in this water potential that creates a 'continuum' within the soil–plant–atmosphere system, despite the phase change from liquid water to vapor within the leaves [2,4,11]. The initial focus is on time scales ranging from sub-hourly to the growing season so that the transport equations can be effectively treated as quasi-stationary in the atmospheric compartment (i.e., the atmospheric scalars equilibrate rapidly with fluxes and sources/sinks), while the temporal dynamics of soil and plant water are explicitly accounted for. At these scales, all plant hydraulic parameters can be assumed constant for a given plant species or functional type and ecosystem. The spatial domain considered here goes from just below the root-zone depth all the way to the atmospheric surface layer above the canopy, with liquid water moving from the soil pores to the roots, and then through plant tissues to the leaves, where it evaporates and diffuses into the atmosphere. Symbols are defined in Fig. 1 and Table 1.

2.1. Soils

Water transport in unsaturated soils is conventionally described by the combination of mass conservation and Darcy's law for unsaturated conditions [12,15,16]. Conservation of mass for water in an unsaturated medium characterized by soil moisture θ_S (and assuming z is positive upwards) is given as

$$\frac{\partial \theta_S}{\partial t} = -\frac{\partial F_S}{\partial z} - \rho_R E_R, \tag{1}$$

where the sink term ($-\rho_R E_R$) represents water uptake by roots, ρ_R is the root area density (∂RAI/∂z, where RAI is the root area index), and E_R is the uptake rate per unit root area. Typically, ρ_R declines monotonically with soil depth [39], whereas E_R depends on the water potential difference between the soil and the root and may thus be positive (water uptake) or negative, when water taken up in deep, moist layers is redistributed to the drier surface soil [40,41]. The vertical water flux in the soil is given as

$$F_S = -k_S(\theta_S)\frac{\partial H}{\partial z}, \tag{2}$$

where the total head is $H = \psi_S(\rho_w g)^{-1} + z$, ψ_S is the soil matric potential, $\rho_w g$ is the specific weight of water (the product of water density, ρ_w, and gravitational acceleration, g), and k_S the soil hydraulic conductivity. Combining Eqs. (1) and (2), and expressing water content in terms of water potential ψ_S results in [42,43]

$$C_S(\psi_S)\frac{\partial \psi_S}{\partial t} = \frac{\partial}{\partial z}\left[k_S(\psi_S)\left(\frac{1}{\rho_w g}\frac{\partial \psi_S}{\partial z} + 1\right)\right] - \rho_R E_R, \tag{3}$$

where $C_S(\psi_S) = d\theta_S/d\psi_S$ is the specific soil moisture capacity [16]. Hydraulic conductivity and water retention curves are typically obtained from empirical relationships [44–49]. The simplest formulations are given as power laws

$$\psi_S = \psi_{S,sat}\left(\frac{\theta_S}{n}\right)^{-b}, \tag{4}$$

$$k_S(\psi_S) = k_{S,sat}\left(\frac{\psi_{S,sat}}{\psi_S}\right)^{2\left(1+\frac{1}{b}\right)}, \tag{5}$$

where $k_{S,sat}$ and $\psi_{S,sat}$ are respectively the soil hydraulic conductivity and water potential near saturation, n is the soil porosity, and b is the exponent of the water retention curve, which is related to pore architecture [50,51].

Upon integration of Eq. (1) in the vertical direction over the entire rooting depth Z_R, a vertically-averaged soil moisture value, $\bar{\theta}_S = Z_R^{-1}\int_0^{Z_R}\theta_S\,dz$, is obtained (where the overbar denotes the vertically-averaged quantities). Based on this vertically averaged soil moisture, a lumped representation of the soil water balance can be derived as [52–54],

$$Z_R\frac{\partial \bar{\theta}_S}{\partial t} = R(t) - Q(\bar{\theta}_S, t) - E_S(\bar{\theta}_S) - E(\bar{\theta}_S) - L(\bar{\theta}_S), \tag{6}$$

where R is the rainfall input, Q is the surface runoff, E is the transpiration flux ($E = \int_0^{Z_R}\rho_R E_R\,dz$), E_S is the water evaporation from the soil, and L is the drainage flux below Z_R (all fluxes in the soil water balance are expressed on a per unit ground area basis).

The flow of water from the soil to the root occurs due to the water potential gradient maintained by the transpiration stream.

Table 1
Definition of symbols. Subscript $i = S, R, P, L$, and A (uppercase letters) indicate soil, root, plant conducting tissue, leaf, and atmospheric compartments, respectively; *max* refers to maximum conductance or rate, *sat* to soil pore saturation or water vapor saturation; overbar indicates vertically-averaged quantities.

Symbol	Definition	Units
a	Shape parameter of the vulnerability curve	–
A_{max}	Maximum photosynthetic rate	μmol m^{-2} s^{-1}
b	Exponent of the water retention curve	–
C_i	Soil or plant hydraulic capacitance ($C_i = \partial\theta_i/\partial\psi_i$)	Pa^{-1}
d_R	Fine root diameter	m
D	Vapor pressure deficit	mol mol^{-1}
E	Transpiration per unit ground area	m s^{-1} or mol m^{-2} s^{-1}
E_L, E_R	Leaf- and root-area specific transpiration rates	m s^{-1} or mol m^{-2} s^{-1}
E_S	Soil evaporation	m s^{-1}
k_i	Hydraulic conductivity of compartment i	m s^{-1}
$k_{P,sap}$, $k_{P,leaf}$	Sapwood- and leaf-specific xylem hydraulic conductivity	kg m^{-1} MPa^{-1} s^{-1}
k_t	Turbulent diffusivity	m^2 s^{-1}
F_i	Vertical water flux	m s^{-1} or mol m^{-2} $^{-1}$
g	Gravitational acceleration	m s^{-2}
g_{bl}	Leaf boundary layer conductance	mol m^{-2} s^{-1}
g_i, $g_{i\text{-}j}$	Hydraulic conductance of compartment i or between i and j	m Pa^{-1} s^{-1} or mol m^{-2} s^{-1}
g_s	Stomatal conductance (note lowercase s)	mol m^{-2} s^{-1}
g_c	Effective canopy conductance ($g_c = \int_0^h \rho_L g_{L-A}dz$)	mol m^{-2} s^{-1}
h	Canopy height	m
H	Total head	m
L	Water leakage below the rooting zone	m s^{-1}
LAI	Leaf area index	m^2 m^{-2}
$\ell_{S\text{-}R}$	Path length between bulk soil and fine roots	m
ℓ_A	Atmospheric mixing length	m
M_w, M_a	Molar mass of water (M_w =0.018) and air (M_a=0.029)	kg mol^{-1}
n	Soil porosity	m^3 m^{-3}
Q	Surface runoff	m s^{-1}
R	Rainfall	m s^{-1}
RAI	Root area index	m^2 m^{-2}
SAI	Sapwood area index	m^2 m^{-2}
s_i	Relative volumetric water content ($= \theta_i/n_i$)	–
Sc	Turbulent Schmidt number	–
T_L	Leaf temperature	°C
U	Horizontal wind speed	m s^{-1}
w_i	Water vapor concentration	mol mol^{-1}
z	Vertical coordinate (positive upwards)	m
Z_R	Rooting depth	m
ρ_L, ρ_R	Leaf and root area densities (=∂LAI/∂z and ∂RAI/∂z)	m^2 m^{-3}
ρ_w	Density of liquid water	kg m^{-3}
θ_i	Volumetric water content	m^3 m^{-3}
ψ_i	Water potential	Pa
ψ_{50}	Water potential at 50% loss of conductivity	Pa

In this lumped representation, water uptake is thus described by diffusion through the soil around the absorbing area of the root, as $E = g_{S\text{-}R}(\overline{\psi_S} - \overline{\psi_R})$. As a first approximation, the soil–root conductance per unit ground area, $g_{S\text{-}R}$ (m s^{-1} Pa^{-1}), can be calculated as [55]

$$g_{S\text{-}R} = \frac{k_S(\overline{\psi_S})}{\rho_w g \ell_{S\text{-}R}}, \tag{7}$$

where $k_S(\overline{\psi_S})$ is the soil hydraulic conductivity (m s^{-1}; Eq. (5)), $\ell_{S\text{-}R}$ is the characteristic length between the bulk soil and the root surface (m), and $\rho_w g$ converts the conductance units to m s^{-1} Pa^{-1}. The distance $\ell_{S\text{-}R}$ can be estimated in different ways depending on root geometry [56–58]. Assuming parallel cylindrical roots of average diameter d_R, uniformly distributed over the depth Z_R, and with a total root area index RAI (m^2 of root surface per m^2 of ground), the characteristic length $\ell_{S\text{-}R}$ is obtained as $\ell_{S\text{-}R} = \sqrt{d_R Z_R \mathrm{RAI}^{-1}}$. Eq. (7) shows the effects of key geometrical parameters (in terms of rooting depth and density of fine absorbing roots, which in turn change with plant type and climate), separately from the ones due to soil moisture and soil hydraulic conductivity. RAI and Z_R vary across biomes (Table 2), and depend on the depth of the bedrock as well as soil and plant type. The root diameter (d_R) is instead more constrained, ranging from around 0.2 mm in grasses to 0.6 mm in trees [59,60].

2.2. Plant tissues

Water transport in the plant tissues (from the root surface to the leaf cuticle and inner surface of the stomatal cavity) can be treated, in analogy with flow in unsaturated soils, as driven by capillary and gravitational gradients [61,62] as

$$C_P(\psi_P)\frac{\partial \psi_P}{\partial t} = \frac{\partial}{\partial z}\left[k_P(\psi_P)\left(\frac{1}{\rho_w g}\frac{\partial \psi_P}{\partial z} + 1\right)\right] - \rho_L E_L, \tag{8}$$

where ψ_P is the water potential inside the plant tissue, k_P is the plant hydraulic conductivity, the capacitance $C_P(\psi_P) = d\theta_P/d\psi_P$ links tissue saturation level and water potential (as before), ρ_L is the leaf area density ($\partial \mathrm{LAI}/\partial z$), and E_L the transpiration per unit leaf area. Note that fluxes and conductivities are here expressed on a ground area basis in analogy with Eq. (3). While the solution of Eq. (8) is affected by the geometry of the plant conductive tissue (branch and root architecture), for simplicity here we neglect these geometric features and focus on the mean properties of the whole plant. Also, the traits controlling water flow (k_P and C_P) as well as sapwood and leaf area indices (SAI and LAI, respectively) are assumed to be representative of the whole plant community, so that Eq. (8) effectively characterizes the mean behavior of the ecosystem.

The capacitance C_P has been estimated experimentally from the slope of the water retention curves in stems [63,64] and leaves [65–70]. Alternatively, C_P can also be estimated from time series analysis of transpiration and sap flow [71]. In general, the xylem hydraulic conductivity $k_P(\psi_P)$ decreases nonlinearly with xylem water potential due to cavitation and embolism formation [9,17]. The shape of $k_P(\psi_P)$, commonly referred to as cavitation vulnerability curve, depends on plant species, although some general patterns can be found, as discussed in Section 3. Vulnerability curves have sigmoidal shape and can typically be described by Weibull functions or similar functional dependencies, such as

$$k_P(\psi_P) = k_{P,max}[1 + (\psi_P/\psi_{50})^a]^{-1}, \tag{9}$$

where $k_{P,max}$ is the maximum xylem hydraulic conductivity (m s^{-1}), a is a shape parameter, and ψ_{50} represents the leaf water potential at 50% loss of conductivity. For laminar flow in a circular vessel, the Hagen–Poiseuille law predicts that hydraulic conductivity should scale as the fourth power of the radius [8,9]. In reality, however, the xylem is composed of vessels of various sizes connected by inter-vessels pits, making it complicated to characterize the microscopic hydraulic features of the conducting tissue. As a consequence, it is often more convenient to measure conductivity at the macroscopic scale (i.e., from stem segments), from which $k_{P,max}$ can be computed in different ways depending on the available data [9]. If leaf-specific conductivity $k_{P,leaf}$ (kg m^{-1} MPa^{-1} s^{-1}) is known, the maximum conductivity (m s^{-1}) can be calculated as $k_{P,max} = k_{P,leaf}g\mathrm{LAI}/10^6$; when the sapwood-specific conductivity $k_{P,sap}$ (kg m^{-1} MPa^{-1} s^{-1}) is provided, $k_{P,max} = k_{P,sap}g\mathrm{SAI}/10^6$. Fig. 2 shows how these hydraulic parameters ($k_{P,sap}$, ψ_{50}, and the shape factor a in Eq. (9)) vary across plant functional types (PFT) and biomes. It should be noted that Eq. (9) is an approximate representation of tension effects on conductivity, which neglects possible hysteretic behavior, caused by delayed recovery of hydraulic conductivity upon pressurization and repair of embolized tissues [72,73].

To reduce Eq. (8) to a lumped model, a homogenous conductive tissue of length h (a measure of the average hydraulic length within the plant, in turn linked to canopy height; e.g., [74]) is assumed along with a homogeneous SAI. Furthermore, all transpired water is assumed to exit the plant at the upper boundary (according to a big-leaf approximation), where tissue water potential is equal to leaf water potential ψ_L. Accordingly, Eq. (8) can be integrated vertically to obtain the plant tissue water balance per unit ground area as

$$h\frac{d\bar{\theta}_P}{dt} = g_{S\text{-}R}(\overline{\psi_S} - \overline{\psi_R}) - E. \tag{10}$$

Assuming steady state conditions ($d\overline{\theta_P}/dt = 0$, i.e., changes in water stored in the plant tissues are small compared to the total transpiration flux) and considering a mean water flux in the xylem ($F_P = -k_P(\overline{\psi_P})\Delta H/h$), transpiration can be obtained from the continuity condition as a function of plant conductance and water potential difference between the root and the leaf [4,20,27,65,74,75],

$$E = g_{R\text{-}L}(\overline{\psi_P})(\overline{\psi_R} - \overline{\psi_L} - \rho_w g h), \tag{11}$$

where $g_{R\text{-}L}(\overline{\psi_P})$ (m Pa^{-1} s^{-1}) is the macroscopic root-to-leaf conductance, which equals the average $k_P(\overline{\psi_P})/(\rho_w g h)$ in this lumped representation. Not only Eq. (11) is used in hydrologic models, but it also often employed in coupled biogeochemical-hydrologic models to link the water potentials of the soil and the canopy, which in turn affects photosynthesis [56,76,77].

Eqs. (8) and (10) are horizontally averaged (thus neglect branching and root architecture) and interpreted as representative of the whole plant community. From the point of view of plant hydraulics, the changes in conductive tissue area and vessel geometry at the internodes from the main stem to the petioles and leaves may be important. Shinozaki et al. [78] proposed a 'pipe model', where each pipe supports structurally and functionally a unit of leaf area. This model implies that the cross sectional area of conductive tissue should be conserved along the plant [37], a law which was first

Table 2
Biome-level mean root area index (RAI), mean rooting depth (Z_r), and maximum rooting depth ($Z_{r,max}$) [39,59,177].

Biome	RAI (m^2 m^{-2})	Z_r(m)	$Z_{r,max}$(m)
Tundra	5.2	0.11	0.5
Boreal forest	4.6	0.17	2.0
Temperate conifer forest	11	0.41	3.9
Temperate deciduous forest	9.8	0.29	2.9
Temperate grassland	79.1	0.17	2.6
Cropland	–	0.25	2.1
Mediterranean shrubland and woodland	11.6	0.27	5.2
Tropical dry forest	6.3	0.25	3.7
Tropical grassland/savanna	42.5	0.35	15.4
Tropical evergreen forest	7.4	0.26	7.3
Desert and semi-desert	5.5	0.39	9.5

predicted by Leonardo Da Vinci. Other approaches assume that plants evolved to maximize hydraulic transport for a given carbon investment in vessel walls, i.e., Murray's law applied to plant tissue [34,79]. In such a case, assuming laminar flow in the vessels, the third power of the vessel radius would be conserved along the branching network. It can be shown that the same arguments leading to Murray's law reproduce the Da Vinci's law if the velocity distribution within the vessels is assumed to be uniform. These relationships affect the hydraulic properties of an individual at a given time. However, when modeling stand development over annual to decadal time scales, the geometry of the system changes (within constraints set by allometric rules), thus affecting the hydraulic architecture of the trees. To account for such changes, models developed to describe stand growth [80–82] can be coupled to the water transport equations, thus providing consistent geometric constraints to the SPAC [57,83].

The interpretation of Eq. (8) at the whole plant community level may be too simplified where species composition and age (and size) structure are important, as in some natural, highly heterogeneous systems. In these cases, the derivation of Eq. (10) would require the proper accounting of these additional sources of spatial (and functional) variability, either through an individual- or functional type-based approach (possibly involving competition) [53,81], or by assuming realistic distributions of parameters and integrating the water transport equations over the parameter space (thus neglecting competition). Heterogeneity in plant size can be accounted for by considering allometric relationships linking resource constraints to the density of individuals and their size and age structure [38,84–86].

2.3. The plant–atmosphere interface

In general, transpiration rate is controlled by a driving force imposed by the atmospheric water demand (driven by solar radiation and air temperature) and the actual water availability in the stomatal cavity, as well as by stomatal conductance, which regulates water losses from the leaves [2]. Simple demand-controlled descriptions of transpiration rate (e.g., [87,88]) may be a good approximation when leaf conductance is not limiting (i.e., under well watered conditions), while stomatal control becomes important under dry conditions. At the leaf level, transpiration per unit leaf area (typically expressed in mol m^{-2} s^{-1}) can be described by Fickian diffusion [3,89],

$$E_L = g_{L\text{-}A}[w_L(\psi_L, T_L) - w_A(T_A)], \tag{12}$$

where $w_L(\psi_L,T_L)$ and $w_A(T_A)$ are water vapor molar concentrations (related to the specific humidity $q = wM_w/M_a$) in equilibrium with the leaf water potential at the leaf temperature T_L and in the bulk atmosphere (at temperature T_A), respectively (molar fluxes can be multiplied by $M_w = 0.018$ kg mol^{-1} and divided by ρ_w to obtain units consistent with Eqs. (3) and (8)). The water vapor difference $w_L(\psi_L,T_L) - w_A(T_A)$ represents the driving force for evaporation from the leaves and corresponds to the atmospheric water pressure deficit (D) when saturation conditions exist inside the stomatal cavity (i.e., $\psi_L \approx 0$) and leaf temperature is close to the air temperature (i.e., $D \approx w_{L,sat}(T_A) - w_A(T_A)$). The vapor pressure difference is determined by compound effects of synoptic-scale dynamics and local-scale water and energy balances. Within canopies, humidity is impacted by transpiration and the atmospheric condition above the canopy, whereas solar radiation alters the leaf energy balance and hence T_L. The effect of solar radiation in turn depends on the leaf surface properties (determining the absorbed radiation) and its size and shape (affecting heat exchange), as well as the atmospheric conditions (e.g., wind speed; see for details [1,65,90]).

In Eq. (12), $g_{L\text{-}A}$ is the leaf–atmosphere conductance, computed from the series of stomatal (g_s) and leaf boundary layer (g_{bl}) conductances, i.e., $g_{L\text{-}A} = g_s g_{bl}/(g_s + g_{bl})$. In turn, g_{bl} can be calculated for any position inside the canopy as a function of mean wind speed and leaf characteristic size, often using flat-plate boundary layer theory [90]. Stomatal conductance responds to environmental fluctuations by decreasing as atmospheric vapor pressure deficit increases and leaf water potential becomes more negative,

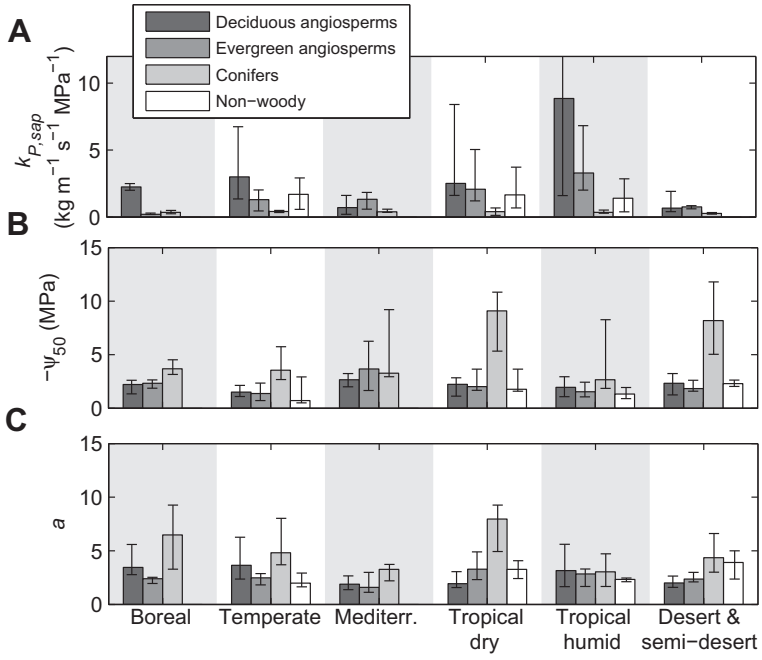

Fig. 2. Median values (with bar indicating first and third quartiles) of (A) sapwood-specific hydraulic conductivity, $k_{P,sap}$, (B) leaf water potential corresponding to 50% loss of conductivity, ψ_{50}, and (C) shape factor for the vulnerability curve, a (Eq. (9)), for major plant functional types and climates (data sources are listed in Table S1 in the online Supplementary materials).

while it increases with light availability [18,19,21,91–93]. To describe these effects, empirical models based on regression of observations [20] or on the observed correlation between photosynthesis and stomatal conductance [94,95] have been developed, providing an empirical link between the plant water and C economies in the form $g_s \sim A/c_a f(D)$, where A is the net photosynthesis, c_a the atmospheric CO_2 concentration, and $f(D)$ a monotonically decreasing function of the vapor pressure deficit D. More mechanistic approaches detail the mechanical movement of guard cells in response to changes in the local pressure [21,96–98], or account for long-distance control from root-derived phyto-hormones, like abscisic acid (ABA) [58,97,99]. These mechanistic models are not yet backed up by sufficient observational data to parameterize them across species and environmental conditions. Approaches based on the postulate that stomata regulate water losses to maximize photosynthesis for a given amount of available soil water represent a viable alternative, thereby eliminating the need to describe the details of the mechanical movement or the signaling mechanism generating the movement of a stoma [100–105]. These optimization models often result in compact analytical expressions for g_s as a function of environmental variables (vapor pressure deficit, atmospheric CO_2 concentration, light and water availability), making them suitable for leaf- to ecosystem-scale applications [106–108]. Using this approach, the scaling of optimal g_s with vapor pressure deficit, CO_2 concentration, light availability, and photosynthetic capacity ($g_s \sim A/\sqrt{c_a D}$) emerges as a result of the optimization hypothesis, lending support to the idea that stomatal responses co-evolved with the plant C economy.

2.4. Atmosphere

For a stationary, high Peclet number and horizontally homogeneous turbulent flow and in the absence of subsidence, the mean mass balance for water vapor within a layer of thickness dz inside the canopy volume can be expressed as

$$\frac{\partial F_A}{\partial z} = \rho_L E_L, \tag{13}$$

where the vertical variation of the mean turbulent flux F_A (mol m^{-2} s^{-1}) is balanced by the local source term $\rho_L E_L$ (leaf transpiration, see Eq. (12)). Eq. (13) can be solved with a prescribed evaporation flux from the soil and a fixed atmospheric water vapor concentration above the canopy as boundary conditions. The most primitive approximation to the turbulent flux can be obtained through a first order-closure scheme given as

$$F_A = -k_t \frac{\partial w_A}{\partial z}, \tag{14}$$

where the turbulent diffusivity k_t can be described as

$$k_t = \frac{\ell_A^2}{Sc}\left|\frac{\partial U}{\partial z}\right|, \tag{15}$$

with Sc being the turbulent Schmidt number and ℓ_A the effective mixing length for turbulence within the canopy, which is in turn controlled by the canopy height and the centroid of the drag force [108,109].

The driving force for transpiration, the vapor pressure difference at the leaf surface $w_L(\psi_L, T_L) - w_A(T_A)$ (Eq. (12)), is also linked to the leaf energy balance and the water vapor concentration profiles (from Eq. (13)). Eqs. (12) and (13) can be further coupled with a mass balance for atmospheric CO_2 concentration, resulting in a complete model of canopy-atmosphere gas and energy exchanges [83,107,108,110,111]. Moreover, a number of schemes have already been proposed to replace Eq. (15) using higher-order closure principles [111], which are advantageous when the scalar flux production term is not locally balanced by its dissipation rate [112].

By vertically integrating Eq. (13), a lumped representation of canopy fluxes can be derived as [41,108,113],

$$F_A(h) = F_A(0) + \int_0^h \rho_L g_{L\text{-}A}(w_L - w_A)dz, \tag{16}$$

where w_A depends on turbulent transport inside the canopy and $g_{L\text{-}A}$ is primarily controlled by light availability. Assuming that gradients in $g_{L\text{-}A}$ in the canopy are much stronger than gradients in w_A, and that the driving force can be approximated by the vapor pressure deficit D, canopy-scale transpiration (in mol m^{-2} s^{-1}) can be calculated from Eq. (16) as

$$E = F_A(h) - F_A(0) = g_c D, \tag{17}$$

where $g_c = \int_0^h \rho_L g_{L\text{-}A}\, dz$ is the effective canopy conductance. Eq. (17) represents the big-leaf approximation of the evaporative demand from the canopy, which is met by the water supply described by Eq. (10). While Eq. (13) allows a more physically-based representation of canopy dynamics, Eq. (17) recovers the diffusion equation formalism and because of its simplicity may be more suitable for large-scale applications [113]. The main limitation of Eq. (17) is the loss of a clear physical and physiological meaning for the canopy conductance g_c, where aerodynamic and stomatal conductances cannot be easily separated.

3. Coordination of hydraulic features and plant function

Because of the tight coupling between transpiration and CO_2 uptake, it is reasonable to expect that vegetation evolved, adapting to the most typical hydro-climatic conditions, toward a coordinated system that effectively transports water and nutrients, while creating the greatest opportunity for carbon uptake and biomass survival, growth, and reproduction. Different aspects of this coordination between the biotic and abiotic components of the ecosystem in relation to the above framework are discussed below focusing on macroscopic plant properties appearing in the lumped description of the SPAC. The observed patterns in these plant parameters across ecosystems and plant functional types (PFT) are thus interpreted as resulting from evolutionary-scale dynamics leading to optimal plant form and function.

3.1. Coordination of plant hydraulic traits within the SPAC

Following the electrical analogy, water transport through the SPAC is controlled by a series of conductances that link the soil to the leaves (Fig. 1). The relative magnitude of these conductances and how they change as a function of water potential determine both the water flux and the pressure gradient through the plant. In electric circuit networks with resistances in series and with nearly stable potential differences, the current (or flow) is larger when the overall resistance is equally partitioned among the different components. In this way, no component constrains the flow more than the others and the overall efficiency is improved. This is also the case in plants, where the acceptable range of water potential drops is limited to avoid damages due to cavitation or excessive leaf heating. Hence, it is reasonable to hypothesize that the maximum conductances (under well-watered conditions) in different parts of the SPAC are inter-related or coordinated, such that a relatively more efficient stem water transport system corresponds to hydraulically-efficient leaves and higher maximum stomatal conductance [29]. In turn, a hydraulically-efficient system provides a competitive advantage because it allows exploiting the available water resources faster than the competing species [53,114–116]. Experimental evidence supports this maximization hypothesis, showing strong correlations between liquid- and vapor-phase (stomatal) conductances [26–28,30,33,117–119] and among leaf

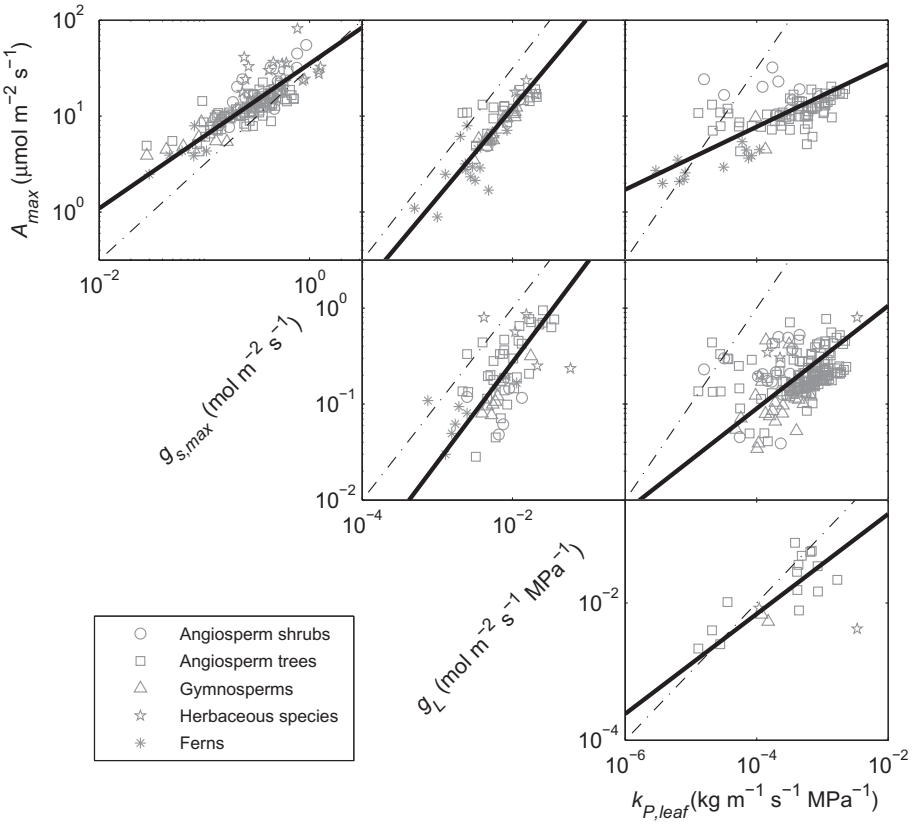

Fig. 3. Correlations among plant traits suggesting evolutionary convergence towards a balanced water–carbon economy: A_{max}, maximum photosynthetic rate; $g_{s,max}$, maximum stomatal conductance; g_L, liquid-phase leaf conductance, and $k_{P,leaf}$, maximum leaf-specific xylem conductivity (data sources are listed in Table S1). Thick solid lines are reduced major axis regressions of the log-transformed data, lines with unitary slope (dot-dashed) are also shown for reference.

lamina, petiole, and whole plant conductances [120]. A review of published values of maximum stomatal conductance, leaf-specific xylem conductivity ($k_{P,leaf}$), and maximum liquid-phase leaf conductance (g_L) showed strong correlations across plant growth forms and climates (Fig. 3). The correlations are all strongly significant ($P < 0.001$, despite some variability due in part to time and method of measurement) except for the weaker relationship between $k_{P,leaf}$ and g_L, for which, however, only few data points are available ($P = 0.0073$).

Moreover, the maximum transpiration rate that can be sustained by the xylem is consistent with measured maximum rates of transpiration, indicating a general coordination between conductances in the water supply system (root to leaf) and at the leaf–atmosphere interface where the water flux is controlled by atmospheric demand and stomatal conductance [29,121–123]. The emergence of this coordination can be illustrated using Eq. (11), where transpiration increases as the leaf water potential becomes more negative. At the same time, however, declining potentials in the xylem cause cavitation and limit further increases in E [29,124]. As a consequence, E is maximized at intermediate ψ_L. This maximum E can be shown to scale linearly with $k_{P,max}$ and ψ_{50} [122], where ψ_{50} decreases with increasing conductivity (Fig. 5). As a result, the maximum E scales nonlinearly with $k_{P,max}$ (with exponent lower than one), so that, using Eq. (12) and assuming a prescribed vapor pressure deficit, we obtain the nonlinear scaling between $k_{P,max}$ and $g_{s,max}$ (Fig. 3).

3.2. Tradeoffs between hydraulic traits during drought

When water becomes limiting, however, both stomatal and xylem conductances are reduced with respect to well-watered conditions. A pressure drop induced by cavitation *causes* stomatal closure by altering the pressure balance between guard and epidermal cells [18,21,97]. However, stomatal closure may be initiated earlier in response to accumulation of ABA that is released by the roots when soil and root water potentials decline [58,99,125]. Increased stomatal sensitivity to low water potential due to ABA reduces transpiration, thus *preventing* catastrophic runaway cavitation, which may result in severe consequences for the whole plant [22,75,99,121,123]. As a result of these reductions in conductances, midday transpiration decreases as drought progresses (Fig. 4a). In some species, the control is primarily through stomatal closure, i.e., the plant water potential at 90% stomatal closure corresponds to a relatively minor loss of xylem conductivity due to cavitation. In other species, such as *Fraxinus excelsior* (Fig. 4b), substantial cavitation may be acceptable and hence stomatal closure is delayed. Based on these different responses and the sets of traits that cause them, plants can be classified as 'cavitation-risk averse' (stomatal closure prevents cavitation maintaining a relatively high midday ψ_L) and 'cavitation-risk tolerant' (stomatal closure and xylem loss of conductivity occur in a more synchronous way) resulting in water transport maximization [8].

Cavitation-risk averse species tend to be isohydric, while the risk tolerant species often show anisohydric behavior [92,99,117,126]. Due to stomatal closure, isohydric species lower the risk of hydraulic failure at the expense of decreased C gain during water stress, possibly leading to C starvation and mortality. In contrast, anisohydric species are more likely to face hydraulic failure before C starvation occurs [22]. As shown in Fig. 4c, conifers tend to be more risk-averse than angiosperms, although inter-specific variability is large within both groups (conifers also tend to have lower absolute values of g_s, as shown in Fig. 3). In fact, not

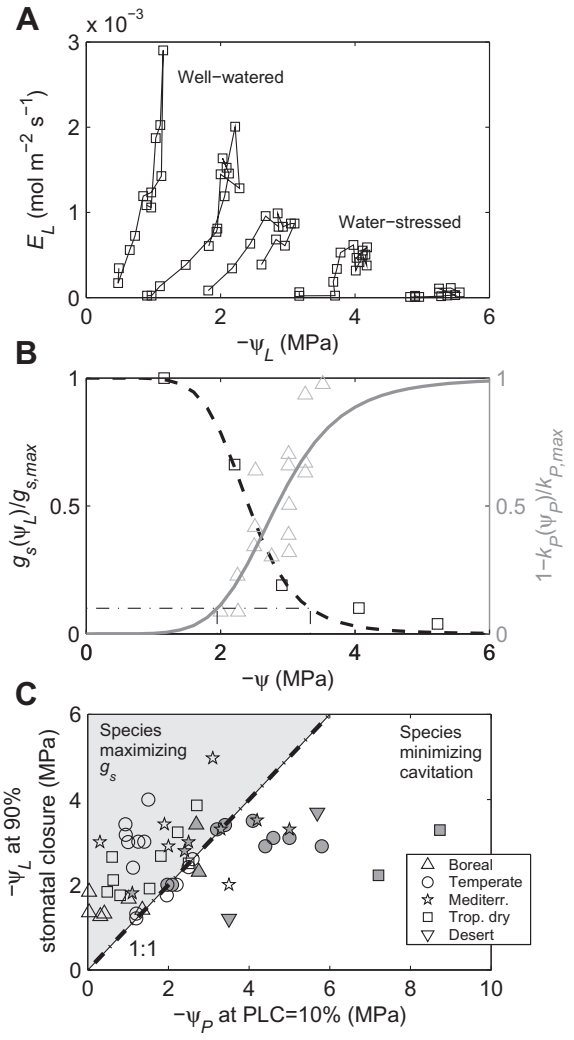

Fig. 4. Relationships between stomatal closure and cavitation-induced loss of conductivity. (A) Leaf-level transpiration as a function of leaf water potential in *Fraxinus excelsior* during days differing in soil water availability from well-watered conditions to severe drought. (B) Changes in stomatal conductance and hydraulic conductivity as a function of water potential (the dot-dashed line refers to 90% stomatal closure and 10% conductivity loss, PLC). (C) Correlation between water potential at PLC = 10% and at 90% stomatal closure for different species (filled symbols refer to conifers, open symbols to angiosperms; shaded and clear areas indicate contrasting water use strategies). Data in A and B are from Carlier et al. [179] and Cochard et al. [180]; data in C from several sources (Table S1).

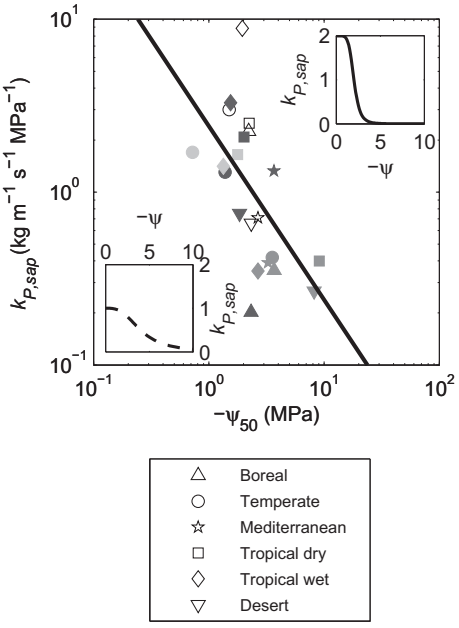

Fig. 5. Inverse correlation between sapwood-specific hydraulic conductivity ($k_{P,sap}$) and water potential at 50% loss of conductivity (ψ_{50}). Data points indicate median values of the parameters (see Fig. 2) for each PFT (open symbols, deciduous angiosperms; dark gray filled, evergreen angiosperms; gray filled, conifers; light gray filled, non-woody species) and climate (legend). Insets show examples of vulnerability curves (Eq. (9)) for 'efficient' (top, solid curve) and 'safe' (bottom, dashed curve) plants; the solid line is the reduced major axis regression of the log-transformed data.

only conifer xylem is more cavitation-resistant (Figs. 2 and 5), but also conifers close their stomata well before cavitation (the water potential at 90% stomatal closure is less negative than the water potential at 10% loss of cavitation, see Fig. 4c). These different behaviors may be related to the higher sensitivity of the evolutionary younger angiosperm stomata, which allow precise regulation close to catastrophic cavitation [127]. Also, different behaviors may emerge in response to the expected water availability, with less conservative water use in species adapted to consistent water supply during the growing season [22,128,129], or in species that face a relatively short (albeit 'uncertain') growing season. This is the case of deciduous species from temperate forests, which transpire and photosynthesize more (per unit ground or canopy area) than conifers at the same site, but over a shorter growing season [130,131].

The level of cavitation-risk tolerance is also apparent in the xylem vulnerability curve, which represents the safety-efficiency tradeoff of the plant conductive tissues. Large hydraulic conductivity is associated with low wood density [132,133] and, more importantly, large vessels with a high number of relatively wide inter-vessel pits that tend to cavitate first as ψ decreases ($k_P \propto r^4$, as from the Hagen–Poiseuille relationship) [134,135]. Accordingly, traits linked to cavitation resistance (ψ_{50}) tend to correlate inversely with maximum hydraulic conductivity ($k_{P,sap}$, see Fig. 5). This safety-efficiency tradeoff is apparent when comparing, in a given climate, the more 'efficient' angiosperms to the 'safer' gymnosperms, but emerges also across biomes (Figs. 2a and 5) [134,136,137]. Larger values of ψ_{50} and $k_{P,sap}$ (and their variability) are observed in climates with strong seasonality (tropical dry and Mediterranean climates), where high efficiency is needed to sustain transpiration during the wet season, while cavitation resistance becomes important at the beginning of the dry season, in particular for evergreen species. Despite strong inverse relationship between ψ_{50} and $k_{P,sap}$ across PFTs and climates, other water use strategies often mask this relationship across species, including phenological responses to drought as well as different stem capacitance and stomatal regulation [23,137–139].

The safety-efficiency tradeoff also emerges within individual plants, along the root–leaf flow path. Roots, stems, and branches are respectively exposed to increasingly more negative leaf water potentials, leading to the expectation that more distal organs should be adapted to the lower ψ_P and hence be less sensitive to changes in water potential and less conductive. Observations confirm this expectation, with lower root ψ_{50} and higher root conductivity than in stems and branches [141–148], although leaves may be more sensitive to cavitation than stems, thus acting as hydraulic 'safety valves' [140].

3.3. Coupling of carbon and water economies

Photosynthesis is intrinsically related to water losses through stomata because diffusion regulates the transport of both CO_2 and water vapor in and out of leaves [149,150]. Stomatal closure in response to changes in the environment thus reduces the supply

of CO_2 and ultimately photosynthesis. Hence, stomata have to balance water savings and carbon uptake demands. Following these economic considerations, Cowan and coworkers hypothesized that stomata act to optimally control gas exchange, so to maximize photosynthesis for a given amount of available soil water [100,151]. The emergent scaling between optimal g_s and A described in Section 2.3 is indicative of this strong C–water interaction.

Because of the coupling between carbon and water fluxes it is expected that the maximum photosynthetic rate (A_{max}) increases proportionally to the hydraulic conductances in the SPAC to guarantee that large water losses are effectively balanced by strong carbon gains [28,30–33,35,55]. This coordination between hydraulic and biochemical systems results in a strong correlations between A_{max} and any measure of water transport efficiency, ranging from leaf to stem conductances (Fig. 3). Such coordination seems to occur not only across species, but also in individuals over time [152,153]. Water flow from the xylem of the leaf veins to the evaporation sites probably causes the larger pressure drop before evaporation because water can only diffuse in the mesophyll tissue. As a consequence, the spatial structure of leaf veins has evolved to supply water in the most efficient way (i.e., minimizing the average distance between the vein and the evaporating site), while limiting unavoidable construction costs [28,154]. These evolutionary tradeoffs led to strong coordination between traits describing leaf venation and C uptake, with higher vein densities occurring in leaves with larger photosynthetic capacity per unit leaf mass and lower leaf mass-to-area ratio [155,156].

The safety-efficiency tradeoff in water transport can also be interpreted as a result of optimal balance between the C gain from leaves that are efficiently supplied by relatively light, but cavitation-sensitive xylem [157], and the C cost of dense wood that is less hydraulically-efficient, but cavitation resistant [132]. Moreover, denser wood has typically lower capacitance and hence provides less water (per unit volume) at times of high demand, with respect to less dense, high capacitance wood [63,64,158]. Hence, lighter wood requires lower C investments and has higher storage capacity, while providing less protection to hydraulic failure. The overall C benefit from these different strategies will ultimately depend on the occurrence of stress events and on the cumulative gas exchange achieved, which are both intrinsically linked to the stochasticity of the rainfall events.

3.4. Whole plant perspective: growth patterns and SPAC

A further degree of freedom to adapt so as to exploit limited resources is provided by the flexibility in allocation between shoots (and thus photosynthesizing tissues) and roots (for water and nutrient uptake), as well as in architectural characteristics (e.g., branching network, canopy shape, root distribution). The hypothesis of balanced development has spawned several models of biomass allocation and growth [159–161]. Among these, allometric theory predicts that water flow in the xylem of individual plants scales with the 3/4 power of total mass, due to the nature of the branch network [37]. Because water supply fuels gross photosynthesis (by means of coupled water–CO_2 transport through stomata and by nutrient uptake), and whole-plant photosynthesis is proportional to the amount of leaves, the theory predicts that total leaf mass should also scale with the 3/4 power of plant mass [84]. Further assuming isometric scaling of plant height and rooting depth leads to the prediction that leaf biomass scales as the 3/4 power of stem and root biomass, in agreement with observations [162], thus supporting the hypothesis of coordinated growth of roots and shoots.

Regarding branching patterns, different approximations have been developed to describe their occurrence, ranging from the so-called pipe model, where the number of conduits does not change with rank in the network [78,163], to Murray's law, where the number of conduits increases with rank [34]. Murray's law is based on the idea that tissues transporting fluids under laminar flow conditions should conserve the third power of conduit radius at internodes to minimize flow resistance and construction costs. This optimal design would allow a competitive advantage and thus would be selected during evolution, as appears to be the case in vascular plants [34]. Root architecture has been studied in much less detail, though a number of studies have shown its importance for hydraulic re-distribution in soils [40,41,164].

The question of growth pattern is further complicated by existing environmental conditions, which may alter the balance of root-to-shoot growth in favor of preferential belowground allocation when water or nutrients are most limiting, or to aboveground structures when light is most limiting. For example, if rooting depth and RAI could be adjusted freely to optimally capture soil water, they would be significantly impacted by rainfall patterns and soil type. Shallow roots would allow exploiting light rainfall events, while deep roots are more suitable to tap deep soil layers that are recharged seasonally or after large rainfall events. The rooting depth that optimally balances investment costs and the need to exploit available water would increase from arid to mesic conditions, but then decrease in wet climates where water is not limiting and shallow roots are sufficient [116,165]. These theoretical predictions are supported by observations worldwide [39,59,166]. Moreover, higher values of RAI are typical of grasslands and savannas, where substantial cover by herbaceous species occurs, and is typical of plants that have lower average rooting depth, possibly to improve intensive water use in the surface soil layer (Table 2). Furthermore, when considering woody species, RAI is highest in temperate climates, while it is lower in both xeric and boreal climates, reflecting lower total biomass in these systems and possibly an economic strategy. In fact, investment costs of high RAI would not be balanced by the relatively small increase in water capture in dry systems with infrequent rain, while such investments are generally not needed in ecosystems that are not water-limited.

Other optimality criteria involving competing water–carbon–nutrient economies can be also hypothesized at the scale of the plant. A large investment in N allows large C uptake at the expense of water losses through transpiration. When water is a limiting factor, however, it becomes necessary for the plant to optimize water use to avoid damage during drought, and hence maximize productivity in the long-term [57,80,167]. Over larger scales, this optimization criteria likely shape vegetation patterns and competition among PFTs [53,114].

4. Challenges and future directions

Despite the progress in understanding the processes controlling water transport through the SPAC, several lines of research remain open regarding both short-term water transport and longer-term changes of vegetation traits in response to climatic variability and change. In particular, further research is needed to mechanistically bridge scales – from xylem pores to the hydraulic traits at the macroscopic scale, and from individuals to communities and ecosystems.

4.1. Scaling up xylem functioning

With regard to the short timescale, the most pressing question is perhaps how micro-scale processes can be represented at the macroscopic scale. While scaling up pore-scale processes in soils has been the subject of much research, little progress has been

made in deriving vulnerability curves from vessel-scale processes, except for a few recent efforts. To progress, a stochastic representation of vessel and inter-vessel pit sizes e.g., [135] could be coupled to a cavitation propagation equation [124], and further linked to the C economy of the plant [157]. Current approaches, however, still neglect vessel network architecture and thus the redundancy of flow paths – a critical hydraulic feature of the xylem. Still subject to debate are also the mechanisms that allow plants to recover from embolism [168–170]. Notably, progress is needed to clarify how recovery time and repair costs depend upon the severity of the cavitation episode and what are the long-term consequences for the whole plant conditions e.g., [35,73].

Soil–root interfaces (at scales spanning μm to mm) are also still poorly characterized. An effective and rigorous way of deriving a macroscopic description based on a representative elementary volume for the soil–root system would improve coupled soil water transport and root uptake models and bridge the gap between 'microscopic' models of water uptake by individual roots and 'macroscopic' approaches consistent with Eq. (3) [42].

4.2. Scaling up to ecosystems

Several challenges also remain when evaluating ecosystem-level water and C fluxes over longer time scales, especially regarding trait coordination and change. The climatic changes expected during the next decades (in particular, intensified precipitation and longer droughts; e.g., [171]) will likely cause shifts in species composition and trigger acclimation responses in the autochthonous populations. For example, plant xylem acclimates to dry conditions by becoming less conductive, but more cavitation-resistant [23,128,148,172], and plant communities may shift towards more drought-adapted species [22,173]. In some cases, different trait combinations may result in similar functional responses due to their inherent tradeoffs (as in Fig. 5), or energy limitation may be more important than plant characteristics, yielding comparable overall fluxes [174,175]. In other cases, species composition may play a more important role and thus alter ecosystem functioning under climatic changes or after disturbance events [131]. Hence, species-specific information is required to capture these changes. However, such level of detail is not always available, so that 'effective', community-level descriptions might be more suitable for wide-scale applications. Mathematical models (coupled to ecosystem-level flux measurements) could improve the quantification of these dynamics by exploring the effects of different community assemblies on the overall fluxes.

Current global climate models employ a functional-type representation of vegetation [176], where each PFT is characterized by a set of traits. A trait-based description of vegetation could represent a more flexible alternative [24,139], where climatic changes may trigger acclimation and alter plant traits, thus affecting ecosystem function (instead of species or PFTs *per se*). This trait-based modeling approach could benefit from a more expansive approach to quantifying causes and outcomes of trait coordination, now possible thanks to recently developed databases (e.g., Table S1 for plant hydraulic traits and TRY initiative for a much wider spectrum of traits, [24]). Plant characteristics in mathematical models could be better constrained by these empirically-based relationships. From a theoretical perspective, predicting trait coordination would yield insights to explain the observed functional and structural patterns as well as their interactions. To proceed in this direction, C, nutrient, and water economies of species or functional groups need to be coupled, thus quantifying plant function and performance from both a biogeochemical and hydrologic perspective. Considering simultaneously all these factors allows defining optimal strategies of resource use that can eventually be linked to the traits and how they correlate. This approach has proved fruitful to predict the general coordination among maximum photosynthesis, leaf lifespan, leaf mass-area ratio, and nitrogen concentration, based on the optimization of water transport [155], and the tradeoffs between xylem safety and efficiency [157]. Within this framework, hydro-climatic stochasticity can not be neglected as it may represent an important constraint over successional-to-evolutionary time scales [36,53]. Thus, the major challenge is now to define optimality criteria and the corresponding optimal states that account for tradeoffs in acquisition and use of resources, as well as for environmental and climatic variability.

Acknowledgements

This work was supported in part by the United States Department of Energy (DOE) through the Office of Biological and Environmental Research (BER) Terrestrial Carbon Processes program (NICCR Grant: DE-FC02-06ER64156) and Terrestrial Ecosystem Science program (DE-SC0006967), the US Department of Agriculture (USDA Grant: 2011-67003-30222), and the National Science Foundation (NSF-CBET-1033467, NSF-EAR-10-13339, NSF-AGS-1102227, NSF-DEB-1145649). We also thank Danielle A. Way, Andrew J. Guswa, and two anonymous reviewers for their constructive comments.

Appendix A. Supplementary data

Supplementary data associated with this article can be found, in the online version, at http://dx.doi.org/10.1016/j.advwatres.2012.03.016.

References

[1] Nobel PS. Physicochemical and environmental plant physiology. Amsterdam, Boston: Academic Press; 2009.
[2] Jarvis PG, Edwards WRN, Talbot H. Models of plant and crop water use. In: Rose DA, Charles-Edwards DA, editors. Mathematics and plant physiology. London: Academic Press; 1981. p. 151–94.
[3] Jarvis PG, McNaughton KG. Stomatal control of transpiration – scaling up from leaf to region. Adv Ecol Res 1986;15:1–49.
[4] van den Honert TH. Water transport in plants as a catenary process. Discuss Faraday Soc 1948;3:146–53.
[5] Tyree MT. The cohesion–tension theory of sap ascent: current controversies. J Exp Bot 1997;48(315):1753–65.
[6] Dixon HH, Joly J. On the ascent of sap. Philos Trans Roy Soc B – Biol Sci 1895;186:563–76.
[7] Boyer JS. Water transport. Annu Rev Plant Physiol Plant Mol Biol 1985;36:473–516.
[8] Cruiziat P, Cochard H, Ameglio T. Hydraulic architecture of trees: main concepts and results. Ann Forest Sci 2002;59(7):723–52.
[9] Tyree MT, Ewers FW. The hydraulic architecture of trees and other woody-plants. New Phytol 1991;119(3):345–60.
[10] Katul G, Porporato A, Oren R. Stochastic dynamics of plant–water interactions. Annu Rev Ecol Evol Syst 2007;38:767–91.
[11] Philip JR. Plant water relations – some physical aspects. Ann Rev Plant Physiol 1966;17:245.
[12] Buckingham E. Studies on the movement of soil moisture. vol. Bulletin 38. Washington, DC: US Department of Agriculture, Bureau of Soils; 1907.
[13] Bonner J. Water transport. Science 1959;129(3347):447–50.
[14] Wheeler TD, Stroock AD. The transpiration of water at negative pressures in a synthetic tree. Nature 2008;455(7210):208–12.
[15] Richards LA. Capillary conduction of liquids through porous mediums. Physics – A J Gen Appl Phys 1931;1(1):318–33.
[16] Hillel D. Environmental soil physics. Academic Press; 1998.
[17] Sperry JS, Stiller V, Hacke UG. Xylem hydraulics and the soil–plant–atmosphere continuum: opportunities and unresolved issues. Agron J 2003;95(6):1362–70.
[18] Buckley TN. The control of stomata by water balance. New Phytol 2005;168(2):275–91.
[19] Oren R, Sperry JS, Katul GG, Pataki DE, Ewers BE, Phillips N, et al. Survey and synthesis of intra- and interspecific variation in stomatal sensitivity to vapour pressure deficit. Plant Cell Environ 1999;22(12):1515–26.
[20] Jarvis PG. Interpretation of variations in leaf water potential and stomatal conductance found in canopies in field. Philos Trans Roy Soc Lond Ser B – Biol Sci 1976;273(927):593–610.
[21] Franks PJ. Stomatal control and hydraulic conductance, with special reference to tall trees. Tree Physiol 2004;24(8):865–78.

[22] McDowell N, Pockman WT, Allen CD, Breshears DD, Cobb N, Kolb T, et al. Mechanisms of plant survival and mortality during drought: why do some plants survive while others succumb to drought? New Phytol 2008;178(4):719–39.
[23] Maseda PH, Fernandez RJ. Stay wet or else: three ways in which plants can adjust hydraulically to their environment. J Exp Bot 2006;57(15):3963–77.
[24] Kattge J, Diaz S, Lavorel S, Prentice C, Leadley P, Bonisch G, et al. TRY – a global database of plant traits. Glob Change Biol 2011;17(9):2905–35.
[25] Stoy PC, Richardson AD, Baldocchi DD, Katul GG, Stanovick J, Mahecha MD, et al. Biosphere–atmosphere exchange of CO_2 in relation to climate: a cross-biome analysis across multiple time scales. Biogeosciences 2009;6(10):2297–312.
[26] Meinzer FC. Co-ordination of vapour and liquid phase water transport properties in plants. Plant Cell Environ 2002;25(2):265–74.
[27] Mencuccini M. The ecological significance of long-distance water transport: short-term regulation, long-term acclimation and the hydraulic costs of stature across plant life forms. Plant Cell Environ 2003;26(1):163–82.
[28] Brodribb TJ, Jordan GJ. Water supply and demand remain balanced during leaf acclimation of *Nothofagus cunninghamii* trees. New Phytol 2011;192(2):437–48.
[29] Sperry JS, Hacke UG, Oren R, Comstock JP. Water deficits and hydraulic limits to leaf water supply. Plant Cell Environ 2002;25(2):251–63.
[30] Franks PJ. Higher rates of leaf gas exchange are associated with higher leaf hydrodynamic pressure gradients. Plant Cell Environ 2006;29(4):584–92.
[31] Brodribb TJ, Feild TS. Stem hydraulic supply is linked to leaf photosynthetic capacity: evidence from New Caledonian and Tasmanian rainforests. Plant Cell Environ 2000;23(12):1381–8.
[32] Meinzer FC. Functional convergence in plant responses to the environment. Oecologia 2003;134(1):1–11.
[33] Santiago LS, Goldstein G, Meinzer FC, Fisher JB, Machado K, Woodruff D, et al. Leaf photosynthetic traits scale with hydraulic conductivity and wood density in Panamanian forest canopy trees. Oecologia 2004;140(4):543–50.
[34] McCulloh KA, Sperry JS, Adler FR. Water transport in plants obeys Murray's law. Nature 2003;421(6926):939–42.
[35] Brodribb TJ. Xylem hydraulic physiology: the functional backbone of terrestrial plant productivity. Plant Sci 2009;177(4):245–51.
[36] Eagleson PS. Ecohydrology. Darwinian expression of vegetation form and function. Cambridge University Press; 2002.
[37] West GB, Brown JH, Enquist BJ. A general model for the origin of allometric scaling laws in biology. Science 1997;276(5309):122–6.
[38] Bejan A, Lorente S, Lee J. Unifying constructal theory of tree roots, canopies and forests. J Theor Biol 2008;254(3):529–40.
[39] Jackson RB, Canadell J, Ehleringer JR, Mooney HA, Sala OE, Schulze ED. A global analysis of root distributions for terrestrial biomes. Oecologia 1996;108(3):389–411.
[40] Jackson RB, Sperry JS, Dawson TE. Root water uptake and transport: using physiological processes in global predictions. Trends Plant Sci 2000;5(11):482–8.
[41] Siqueira M, Katul G, Porporato A. Onset of water stress, hysteresis in plant conductance, and hydraulic lift: scaling soil water dynamics from millimeters to meters. Water Resour Res 2008;44(1):W01432.
[42] Hopmans JW, Bristow KL. Current capabilities and future needs of root water and nutrient uptake modeling. Adv Agron 2002;77:103–83.
[43] Šimůnek J, Hopmans JW. Modeling compensated root water and nutrient uptake. Ecol Model 2009;220(4):505–21.
[44] Clapp RB, Hornberger GM. Empirical equations for some soil hydraulic-properties. Water Resour Res 1978;14(4):601–4.
[45] Cosby BJ, Hornberger GM, Clapp RB, Ginn TR. A statistical exploration of the relationships of soil–moisture characteristics to the physical-properties of soils. Water Resour Res 1984;20(6):682–90.
[46] Campbell GS. Simple method for determining unsaturated conductivity from moisture retention data. Soil Sci 1974;117(6):311–4.
[47] Brooks RH, Corey AT. Hydraulic properties of porous media. In: Hydrology papers. Colorado State University: Fort Collins, CO; 1964. p. 27.
[48] Brutsaert W. Hydrology: an introduction. Cambridge: Cambridge University Press; 2005.
[49] van Genuchten MT. A closed-form equation for predicting the hydraulic conductivity of unsaturated soils. Soil Sci Soc Am J 1980;44(5):892–8.
[50] Mualem Y. Hydraulic conductivity of unsaturated soils: orediction and formulas. In: Campbell GS, Jackson RD, Klute A, Mortland MM, Nielsen DR, editors. Methods of soil analysis. Part I: Physical and mineralogical methods. Madison, WI: American Society of Agronomy, Soil Science Society of America; 1986, p. 799–823.
[51] Mualem Y, Dagan G. Hydraulic conductivity of soils – unified approach to statistical-models. Soil Sci Soc Am J 1978;42(3):392–5.
[52] Laio F, Porporato A, Ridolfi L, Rodriguez-Iturbe I. Plants in water-controlled ecosystems: active role in hydrologic processes and response to water stress – II. Probabilistic soil moisture dynamics. Adv Water Resour 2001;24(7):707–23.
[53] Rodriguez-Iturbe I, Porporato A. Ecohydrology of water-controlled ecosystems. Soil moisture and plant dynamics. Cambridge: Cambridge University Press; 2004.
[54] Rodriguez-Iturbe I, Porporato A, Ridolfi L, Isham V, Cox DR. Probabilistic modelling of water balance at a point: the role of climate, soil and vegetation. Proc Roy Soc Lond Ser A – Math Phys Eng Sci 1999;455(1990):3789–805.
[55] Katul G, Leuning R, Oren R. Relationship between plant hydraulic and biochemical properties derived from a steady-state coupled water and carbon transport model. Plant Cell Environ 2003;26(3):339–50.
[56] Daly E, Porporato A, Rodriguez-Iturbe I. Coupled dynamics of photosynthesis, transpiration, and soil water balance. Part I: Upscaling from hourly to daily level. J Hydrometeorol 2004;5(3):546–58.
[57] Schymanski SJ, Sivapalan M, Roderick ML, Hutley LB, Beringer J. An optimality-based model of the dynamic feedbacks between natural vegetation and the water balance. Water Resour Res 2009;45:W01412.
[58] Tardieu F, Davies WJ. Integration of hydraulic and chemical signaling in the control of stomatal conductance and water status of droughted plants. Plant Cell Environ 1993;16(4):341–9.
[59] Jackson RB, Mooney HA, Schulze ED. A global budget for fine root biomass, surface area, and nutrient contents. Proc Natl Acad Sci USA 1997;94(14):7362–6.
[60] Pregitzer KS, DeForest JL, Burton AJ, Allen MF, Ruess RW, Hendrick RL. Fine root architecture of nine North American trees. Ecol Monogr 2002;72(2):293–309.
[61] Bohrer G, Mourad H, Laursen TA, Drewry D, Avissar R, Poggi D, et al. Finite element tree crown hydrodynamics model (FETCH) using porous media flow within branching elements: a new representation of tree hydrodynamics. Water Resour Res 2005;41(11):W11404.
[62] Aumann CA, Ford ED. Modeling tree water flow as an unsaturated flow through a porous medium. J Theor Biol 2002;219(4):415–29.
[63] Meinzer FC, Woodruff DR, Domec JC, Goldstein G, Campanello PI, Campanello MG, et al. Coordination of leaf and stem water transport properties in tropical forest trees. Oecologia 2008;156(1):31–41.
[64] Scholz FG, Bucci SJ, Goldstein G, Meinzer FC, Franco AC, Miralles-Wilhelm F. Biophysical properties and functional significance of stem water storage tissues in Neotropical savanna trees. Plant Cell Environ 2007;30(2):236–48.
[65] Jones HG. Plants and microclimate. A quantitative approach to environmental plant physiology. Cambridge, NY: Cambridge University Press; 1992.
[66] Machado JL, Tyree MT. Patterns of hydraulic architecture and water relations of 2 tropical canopy trees with contrasting leaf phenologies – ochroma-pyramidale and pseudobombax-septenatum. Tree Physiol 1994;14(3):219–40.
[67] Saha S, Holbrook NM, Montti L, Goldstein G, Cardinot GK. Water relations of Chusquea ramosissima and *Merostachys claussenii* in Iguazu National Park, Argentina. Plant Physiol 2009;149(4):1992–9.
[68] Brodribb TJ, Holbrook NM. Stomatal closure during leaf dehydration, correlation with other leaf physiological traits. Plant Physiol 2003;132(4):2166–73.
[69] Acock B, Grange RI. Equilibrium models of leaf water relations. In: Rose DA, Charles-Edwards DA, editors. Mathematics and plant physiology. London: Academic Press; 1981. p. 29–47.
[70] Loik ME, Harte J. Changes in water relations for leaves exposed to a climate-warming manipulation in the Rocky Mountains of Colorado. Environ Exp Bot 1997;37(2–3):115–23.
[71] Phillips N, Nagchaudhuri A, Oren R, Katul G. Time constant for water transport in loblolly pine trees estimated from time series of evaporative demand and stem sapflow. Trees – Struct Funct 1997;11(7):412–9.
[72] Sperry JS, Tyree MT. Water-stress-induced xylem embolism in 3 species of conifers. Plant Cell Environ 1990;13(5):427–36.
[73] Brodribb TJ, Cochard H. Hydraulic failure defines the recovery and point of death in water-stressed conifers. Plant Physiol 2009;149(1):575–84.
[74] Novick K, Oren R, Stoy P, Juang JY, Siqueira M, Katul G. The relationship between reference canopy conductance and simplified hydraulic architecture. Adv Water Resour 2009;32(6):809–19.
[75] Jones HG, Sutherland RA. Stomatal control of xylem embolism. Plant Cell Environ 1991;14(6):607–12.
[76] Vico G, Porporato A. Modelling C3 and C4 photosynthesis under water-stressed conditions. Plant Soil 2008;313(1–2):187–203.
[77] Williams M, Rastetter EB, Fernandes DN, Goulden ML, Wofsy SC, Shaver G, et al. Modelling the soil–plant–atmosphere continuum in a *Quercus-Acer* stand at Harvard forest: the regulation of stomatal conductance by light, nitrogen and soil/plant hydraulic properties. Plant Cell Environ 1996;19(8):911–27.
[78] Shinozaki K, Yoda K, Hozumi K, Kira T. A quantitative analysis of plant form – the pipe model theory. I: Basic analyses. Jpn J Ecol 1964;14(3):97–105.
[79] Sherman TF. On connecting large vessels to small – the meaning of Murray law. J Gen Physiol 1981;78(4):431–53.
[80] Buckley TN, Roberts DW. DESPOT, a process-based tree growth model that allocates carbon to maximize carbon gain. Tree Physiol 2006;26(2):129–44.
[81] Falster DS, Brannstrom A, Dieckmann U, Westoby M. Influence of four major plant traits on average height, leaf-area cover, net primary productivity, and biomass density in single-species forests: a theoretical investigation. J Ecol 2011;99(1):148–64.
[82] Mäkelä A. A carbon balance model of growth and self-pruning in trees based on structural relationships. Forest Sci 1997;43(1):7–24.
[83] Siqueira MB, Katul GG, Sampson DA, Stoy PC, Juang JY, McCarthy HR, et al. Multiscale model intercomparisons of CO_2 and H_2O exchange rates in a maturing southeastern US pine forest. Glob Change Biol 2006;12(7):1189–207.
[84] Enquist BJ, Brown JH, West GB. Allometric scaling of plant energetics and population density. Nature 1998;395(6698):163–5.

[85] Enquist BJ, Niklas KJ. Invariant scaling relations across tree-dominated communities. Nature 2001;410(6829):655–60.
[86] West GB, Enquist BJ, Brown JH. A general quantitative theory of forest structure and dynamics. Proc Natl Acad Sci USA 2009;106(17):7040–5.
[87] Penman HL. Natural evaporation from open water, bare soil and grass. Proc Roy Soc Lond Ser A – Math Phys Sci 1948;193(1032):120–45.
[88] Priestley CHB, Taylor RJ. Assessment of surface heat-flux and evaporation using large-scale parameters. Mon Weather Rev 1972;100(2):81–92.
[89] Korner C, Scheel JA, Bauer H. Maximum leaf diffusive conductance in vascular plants. Photosynthetica 1979;13(1):45–82.
[90] Campbell GS, Norman JM. An introduction to environmental biophysics. 2nd ed. Springer; 1998.
[91] Monteith JL. A reinterpretation of stomatal responses to humidity. Plant Cell Environ. 1995;18(4):357–64.
[92] Larcher W. Physiological plant ecology. 4th ed. Berlin: Springer; 2003.
[93] Vico G, Manzoni S, Palmroth S, Katul G. Effects of stomatal delays on the economics of leaf gas exchange under intermittent light regimes. New Phytol 2011;192(3):640–52.
[94] Collatz GJ, Ball JT, Grivet C, Berry JA. Physiological and environmental-regulation of stomatal conductance, photosynthesis and transpiration – a model that includes a laminar boundary-layer. Agric Forest Meteorol 1991;54(2–4):107–36.
[95] Leuning R. A critical-appraisal of a combined stomatal-photosynthesis model for C-3 plants. Plant Cell Environ 1995;18(4):339–55.
[96] Buckley TN, Mott KA, Farquhar GD. A hydromechanical and biochemical model of stomatal conductance. Plant Cell Environ 2003;26(10):1767–85.
[97] Dewar RC. The Ball–Berry–Leuning and Tardieu–Davies stomatal models: synthesis and extension within a spatially aggregated picture of guard cell function. Plant Cell Environ 2002;25(11):1383–98.
[98] Gao Q, Zhao P, Zeng X, Cai X, Shen W. A model of stomatal conductance to quantify the relationship between leaf transpiration, microclimate and soil water stress. Plant Cell Environ 2002;25(11):1373–81.
[99] Tardieu F, Simonneau T. Variability among species of stomatal control under fluctuating soil water status and evaporative demand: modelling isohydric and anisohydric behaviours. J Exp Bot 1998;49:419–32.
[100] Cowan I, Farquhar GD. Stomatal function in relation to leaf metabolism an environment. In: Integration of activity in the higher plants. Symposia of the Society of Experimental Biology. Cambridge University Press; 1977.
[101] Hari P, Mäkelä A, Korpilahti E, Holmberg M. Optimal control of gas exchange. Tree Physiol 1986;2:169–75.
[102] Katul G, Palmroth S, Oren R. Leaf stomatal responses to vapour pressure deficit under current and CO_2-enriched atmosphere explained by the economics of gas exchange. Plant Cell Environ 2009;32:968–79.
[103] Konrad W, Roth-Nebelsick A, Grein M. Modelling of stomatal density response to atmospheric CO_2. J Theor Biol 2008;253(4):638–58.
[104] Manzoni S, Vico G, Katul G, Fay PA, Polley W, Palmroth S, et al. Optimizing stomatal conductance for maximum carbon gain under water stress: a meta-analysis across plant functional types and climates. Funct Ecol 2011;25(3):456–67.
[105] Buckley TN, Miller JM, Farquhar GD. The mathematics of linked optimisation for water and nitrogen use in a canopy. Silva Fenn 2002;36(3):639–69.
[106] Mäkelä A, Berninger F, Hari P. Optimal control of gas exchange during drought: theoretical analysis. Ann Bot 1996;77(5):461–7.
[107] Manzoni S, Katul G, Fay PA, Polley HW, Porporato A. Modeling the vegetation-atmosphere carbon dioxide and water vapor interactions along a controlled CO_2 gradient. Ecol Model 2011;222(3):653–65.
[108] Launiainen S, Katul GG, Kolari P, Vesala T, Hari P. Empirical and optimal stomatal controls on leaf and ecosystem level CO(2) and H(2)O exchange rates. Agric Forest Meteorol 2011;151(12):1672–89.
[109] Katul GG, Mahrt L, Poggi D, Sanz C. One- and two-equation models for canopy turbulence. Bound-Layer Meteorol 2004;113(1):81–109.
[110] Baldocchi D, Meyers T. On using eco-physiological, micrometeorological and biogeochemical theory to evaluate carbon dioxide, water vapor and trace gas fluxes over vegetation: a perspective. Agric Forest Meteorol 1998;90(1–2):1–25.
[111] Juang JY, Katul GG, Siqueira MB, Stoy PC, McCarthy HR. Investigating a hierarchy of Eulerian closure models for scalar transfer inside forested canopies. Bound-Layer Meteorol 2008;128(1):1–32.
[112] Cava D, Katul GG, Scrimieri A, Poggi D, Cescatti A, Giostra U. Buoyancy and the sensible heat flux budget within dense canopies. Bound-Layer Meteorol 2006;118(1):217–40.
[113] Raupach MR, Finnigan JJ. Single-layer models of evaporation from plant canopies are incorrect but useful, whereas multilayer models are correct but useless – discuss. Aust J Plant Physiol 1988;15(6):705–16.
[114] Caylor KK, Scanlon TM, Rodriguez-Iturbe I. Ecohydrological optimization of pattern and processes in water-limited ecosystems: a trade-off-based hypothesis. Water Resour Res 2009;45:W08407.
[115] DeLucia EH, Heckathorn SA. The effect of soil drought on water-use efficiency in a contrasting Great-Basin desert and Sierran montane species. Plant Cell Environ 1989;12(9):935–40.
[116] Guswa AJ. Effect of plant uptake strategy on the water-optimal root depth. Water Resour Res 2010;46:W09601.
[117] Sperry JS. Hydraulic constraints on plant gas exchange. Agric Forest Meteorol 2000;104(1):13–23.
[118] Meinzer FC, Goldstein G, Jackson P, Holbrook NM, Gutierrez MV, Cavelier J. Environmental and physiological regulation of transpiration in tropical forest gap species – the influence of boundary-layer and hydraulic-properties. Oecologia 1995;101(4):514–22.
[119] Saliendra NZ, Sperry JS, Comstock JP. Influence of leaf water status on stomatal response to humidity, hydraulic conductance, and soil drought in *Betula-Occidentalis*. Planta 1995;196(2):357–66.
[120] Sack L, Cowan PD, Jaikumar N, Holbrook NM. The 'hydrology' of leaves: co-ordination of structure and function in temperate woody species. Plant Cell and Environ 2003;26(8):1343–56.
[121] Tyree MT, Sperry JS. Do woody-plants operate near the point of catastrophic xylem dysfunction caused by dynamic water-stress – answers from a model. Plant Physiol 1988;88(3):574–80.
[122] Manzoni S, Vico G, Katul G, Palmroth S, Jackson RB, Porporato A. Hydraulic limits on maximum plant transpiration, in preparation.
[123] Sperry JS, Adler FR, Campbell GS, Comstock JP. Limitation of plant water use by rhizosphere and xylem conductance: results from a model. Plant Cell Environ 1998;21(4):347–59.
[124] Meyra AG, Zarragoicoechea GJ, Kuz VA. A similarity law in botanic. The case of hydraulic conductivity of trees. Eur Phys J D 2011;62(1):19–23.
[125] Chaves MM, Maroco JP, Pereira JS. Understanding plant responses to drought – from genes to the whole plant. Funct Plant Biol 2003;30(3):239–64.
[126] Franks PJ, Drake PL, Froend RH. Anisohydric but isohydrodynamic: seasonally constant plant water potential gradient explained by a stomatal control mechanism incorporating variable plant hydraulic conductance. Plant Cell Environ 2007;30(1):19–30.
[127] Sperry JS. Coordinating stomatal and xylem functioning – an evolutionary perspective. New Phytol 2004;162(3):568–70.
[128] Pockman WT, Sperry JS. Vulnerability to xylem cavitation and the distribution of Sonoran desert vegetation. Am J Bot 2000;87(9):1287–99.
[129] Kumagai T, Porporato A. Strategies of a Bornean tropical rainforest water use as a function of rainfall regime: isohydric or anisohydric? Plant Cell Environ 2012;35:61–71.
[130] Catovsky S, Holbrook NM, Bazzaz FA. Coupling whole-tree transpiration and canopy photosynthesis in coniferous and broad-leaved tree species. Can J Forest Res – Rev Can Rech Forest 2002;32(2):295–309.
[131] Hadley JL, Kuzeja PS, Daley MJ, Phillips NG, Mulcahy T, Singh S. Water use and carbon exchange of red oak- and eastern hemlock-dominated forests in the northeastern USA: implications for ecosystem-level effects of hemlock woolly adelgid. Tree Physiol 2008;28(4):615–27.
[132] Hacke UG, Sperry JS, Pockman WT, Davis SD, McCulloch KA. Trends in wood density and structure are linked to prevention of xylem implosion by negative pressure. Oecologia 2001;126(4):457–61.
[133] Chave J, Coomes D, Jansen S, Lewis SL, Swenson NG, Zanne AE. Towards a worldwide wood economics spectrum. Ecol Lett 2009;12(4):351–66.
[134] Hacke UG, Sperry JS, Wheeler JK, Castro L. Scaling of angiosperm xylem structure with safety and efficiency. Tree Physiol 2006;26(6):689–701.
[135] Christman MA, Sperry JS, Adler FR. Testing the 'rare pit' hypothesis for xylem cavitation resistance in three species of Acer. New Phytol 2009;182(3):664–74.
[136] Maherali H, Pockman WT, Jackson RB. Adaptive variation in the vulnerability of woody plants to xylem cavitation. Ecology 2004;85(8):2184–99.
[137] Meinzer FC, McCulloh KA, Lachenbruch B, Woodruff DR, Johnson DM. The blind men and the elephant: the impact of context and scale in evaluating conflicts between plant hydraulic safety and efficiency. Oecologia 2010;164(2):287–96.
[138] Eamus D, Prior L. Ecophysiology of trees of seasonally dry tropics: comparisons among phenologies. Adv Ecol Res 2001;32:113–97.
[139] Goldstein G, Meinzer FC, Bucci SJ, Scholz FG, Franco AC, Hoffmann WA. Water economy of Neotropical savanna trees: six paradigms revisited. Tree Physiol 2008;28(3):395–404.
[140] Johnson DM, McCulloh KA, Meinzer FC, Woodruff DR, Eissenstat DM. Hydraulic patterns and safety margins, from stem to stomata, in three eastern US tree species. Tree Physiol 2011;31(6):659–68.
[141] Martinez-Vilalta J, Prat E, Oliveras I, Pinol J. Xylem hydraulic properties of roots and stems of nine Mediterranean woody species. Oecologia 2002;133(1):19–29.
[142] Froux F, Ducrey M, Dreyer E, Huc R. Vulnerability to embolism differs in roots and shoots and among three Mediterranean conifers: consequences for stomatal regulation of water loss? Trees – Struct Funct 2005;19(2):137–44.
[143] Maherali H, Moura CF, Caldeira MC, Willson CJ, Jackson RB. Functional coordination between leaf gas exchange and vulnerability to xylem cavitation in temperate forest trees. Plant Cell Environ 2006;29(4):571–83.
[144] Willson CJ, Manos PS, Jackson RB. Hydraulic traits are influenced by phylogenetic history in the drought-resistant, invasive genus *Juniperus* (Cupressaceae). Am J Bot 2008;95(3):299–314.
[145] Oliveras I, Martinez-Vilalta J, Jimenez-Ortiz T, Lledo MJ, Escarre A, Pinol J. Hydraulic properties of *Pinus halepensis*, *Pinus pinea* and *Tetraclinis articulata* in a dune ecosystem of Eastern Spain. Plant Ecol 2003;169(1):131–41.
[146] Sperry JS, Saliendra NZ. Intra-plant and inter-plant variation in xylem cavitation in *Betula-Occidentalis*. Plant Cell Environ 1994;17(11):1233–41.
[147] Domec JC, Pruyn ML. Bole girdling affects metabolic properties and root, trunk and branch hydraulics of young ponderosa pine trees. Tree Physiol 2008;28(10):1493–504.
[148] Kolb KJ, Sperry JS. Transport constraints on water use by the Great Basin shrub, *Artemisia tridentata*. Plant Cell Environ 1999;22(8):925–35.
[149] Cowan IR, Troughton JH. Relative role of stomata in transpiration and assimilation. Planta 1971;97(4):325–36.

[150] Farquhar GD, Sharkey TD. Stomatal conductance and photosynthesis. Annu Rev Plant Physiol Plant Mol Biol 1982;33:317–45.
[151] Cowan I. Economics of carbon fixation in higher plants. In: Givnish TJ, editor. On the economy of plant form and function. Cambridge: Cambridge University Press; 1986. p. 133–70.
[152] Noormets A, Sober A, Pell EJ, Dickson RE, Podila GK, Sober GK, et al. Stomatal and non-stomatal limitation to photosynthesis in two trembling aspen (*Populus tremuloides* Michx.) clones exposed to elevated CO2 and/or O-3. Plant Cell Environ 2001;24(3):327–36.
[153] Xu LK, Baldocchi DD. Seasonal trends in photosynthetic parameters and stomatal conductance of blue oak (*Quercus douglasii*) under prolonged summer drought and high temperature. Tree Physiol 2003;23(13):865–77.
[154] Brodribb TJ, Feild TS, Sack L. Viewing leaf structure and evolution from a hydraulic perspective. Funct Plant Biol 2010;37(6):488–98.
[155] Blonder B, Violle C, Bentley LP, Enquist BJ. Venation networks and the origin of the leaf economics spectrum. Ecol Lett 2011;14(2):91–100.
[156] Brodribb TJ, Feild TS, Jordan GJ. Leaf maximum photosynthetic rate and venation are linked by hydraulics. Plant Physiol 2007;144(4):1890–8.
[157] Hölttä T, Mencuccini M, Nikinmaa E. A carbon cost-gain model explains the observed patterns of xylem safety and efficiency. Plant Cell Environ 2011;34(11):1819–34.
[158] Stratton L, Goldstein G, Meinzer FC. Stem water storage capacity and efficiency of water transport: their functional significance in a Hawaiian dry forest. Plant Cell Environ 2000;23(1):99–106.
[159] McCarthy MC, Enquist BJ. Consistency between an allometric approach and optimal partitioning theory in global patterns of plant biomass allocation. Funct Ecol 2007;21(4):713–20.
[160] Niklas KJ, Enquist BJ. On the vegetative biomass partitioning of seed plant leaves, stems, and roots. Am Nat 2002;159(5):482–97.
[161] Thornley JHM, Johnson IR. Plant and crop modelling: a mathematical approach to plant and crop physiology. Oxford: Clarendon Press; 1990.
[162] Enquist BJ, Niklas KJ. Global allocation rules for patterns of biomass partitioning in seed plants. Science 2002;295(5559):1517–20.
[163] West GB, Brown JH, Enquist BJ. A general model for the structure and allometry of plant vascular systems. Nature 1999;400(6745):664–7.
[164] Katul GG, Siqueira MB. Biotic and abiotic factors act in coordination to amplify hydraulic redistribution and lift. New Phytol 2010;187(1):4–6.
[165] Guswa AJ. The influence of climate on root depth: a carbon cost-benefit analysis. Water Resour Res 2008;44(2):W02427.
[166] Schenk HJ, Jackson RB. Rooting depths, lateral root spreads and below-ground/above-ground allometries of plants in water-limited ecosystems. J Ecol 2002;90(3):480–94.
[167] McMurtrie RE, Norby RJ, Medlyn BE, Dewar RC, Pepper DA, Reich PB, et al. Why is plant-growth response to elevated CO_2 amplified when water is limiting, but reduced when nitrogen is limiting? A growth-optimisation hypothesis. Funct Plant Biol 2008;35(6):521–34.
[168] Holbrook NM, Zwieniecki MA. Embolism repair and xylem tension: do we need a miracle? Plant Physiol 1999;120(1):7–10.
[169] Zwieniecki MA, Holbrook NM. Confronting Maxwell's demon: biophysics of xylem embolism repair. Trends Plant Sci 2009;14(10):530–4.
[170] Vesala T, Hölttä T, Peramaki M, Nikinmaa E. Refilling of a hydraulically isolated embolized xylem vessel: model calculations. Annals of Bot 2003;91(4):419–28.
[171] IPCC. Climate change 2007: the physical science basis. In: Solomon S, Qin D, Manning M, Chen Z, Marquis M, Averyt KB, et al., editors. Contribution of working group I to the fourth assessment report of the intergovernmental panel on climate change. Cambridge University Press; 2007.
[172] Fichot R, Barigah TS, Chamaillard S, Le Thiec D, Laurans F, Cochard H, et al. Common trade-offs between xylem resistance to cavitation and other physiological traits do not hold among unrelated *Populus deltoides* × *Populus nigra* hybrids. Plant Cell Environ 2010;33(9):1553–68.
[173] Knapp AK, Beier C, Briske DD, Classen AT, Luo Y, Reichstein M, et al. Consequences of more extreme precipitation regimes for terrestrial ecosystems. Bioscience 2008;58(9):811–21.
[174] Kelliher FM, Leuning R, Schulze ED. Evaporation and canopy characteristics of coniferous forests and grasslands. Oecologia 1993;95(2):153–63.
[175] Stoy PC, Katul GG, Siqueira MBS, Juang JY, Novick KA, McCarthy HR, et al. Separating the effects of climate and vegetation on evapotranspiration along a successional chronosequence in the southeastern US. Glob Change Biol 2006;12(11):2115–35.
[176] Sitch S, Huntingford C, Gedney N, Levy PE, Lomas M, Piao SL, et al. Evaluation of the terrestrial carbon cycle, future plant geography and climate-carbon cycle feedbacks using five Dynamic Global Vegetation Models (DGVMs). Glob Change Biol 2008;14(9):2015–39.
[177] Canadell J, Jackson RB, Ehleringer JR, Mooney HA, Sala OE, Schulze ED. Maximum rooting depth of vegetation types at the global scale. Oecologia 1996;108(4):583–95.
[178] Gollan T, Turner NC, Schulze ED. The responses of stomata and leaf gas-exchange to vapor-pressure deficits and Soil–Water Content. 3: In the sclerophyllous woody species nerium oleander. Oecologia 1985;65(3):356–62.
[179] Carlier G, Peltier JP, Gielly L. Water relations of ash (*Fraxinus-Excelsior* L) in a mesoxerophilic mountain stand. Ann Sci Forest 1992;49(3):207–23.
[180] Cochard H, Peiffer M, LeGall K, Granier A. Developmental control of xylem hydraulic resistances and vulnerability to embolism in *Fraxinus excelsior* L: impacts on water relations. J Exp Bot 1997;48(308):655–63.